Electronic Supplementary Information
(42 pages)

Iridium-Mediated C–S Bond Activation and Transformation: Organoiridium(III) Thioether, Thiolato, Sulfinato and Thiyl Radical Compounds. Synthesis, Mechanistic, Spectral, Electrochemical and Theoretical Aspects

Ujjwal Das, Tapas Ghorui, Basab Adhikari, Sima Roy, Shuvam Pramanik and Kausikisankar Pramanik*

Department of Chemistry, Inorganic Chemistry Section, Jadavpur University, Kolkata – 700032, India.
E-mail: kpramanik@hotmail.com; Tel: +91 94333 66013

Contents

Physical Measurements

The elemental analyses (C, H, N) were performed with a Perkin-Elmer model 2400 series II elemental analyzer. IR spectra were recorded on Perkin-Elmer L-0100 spectrometer with samples prepared as KBr pellets. ^{1}H NMR spectral measurement was carried out on a Bruker FT 300 MHz spectrometer with TMS as an internal reference. ^{31}P NMR spectral measurements were carried out on a Bruker AMX 500 Spectrometer operating at 202.42 MHz. The electrospray ionization mass spectra (ESI-MS positive) were measured in acetonitrile on a Micromass Qtof YA 263 mass spectrometer. The electronic spectra in dichloromethane solution were obtained using a Perkin-Elmer LAMDA 25 spectrophotometer with a solute concentration of about 10^{-4} M. Emission spectra were recorded on Perkin-Elmer LS 55 fluorescence spectrophotometer spectra in dichloromethane solutions at room temperature. Emission quantum yields of the complexes were determined in freeze-pump-thaw-degassed solutions of the complexes by a relative method using anthracene in ethanol as the standard.[1] The emission quantum yield for complexes (Φ_r) was calculated by the well-known equation[2] given below:

$$\Phi_r = \Phi_{std} \frac{A_{std}}{A_r} \frac{I_r}{I_{std}} \frac{\eta_r^2}{\eta_{std}^2} \qquad (1)$$

where Φ_r and Φ_{std} are the quantum yields of unknown and standard samples (Φ_{std}=0.27[3] (at 298 K) in ethanol at λ_{ex} = 341 nm), A_r and A_{std} (< 0.1) are the solution absorbances at the excitation wavelength (λ_{ex}), I_r and I_{std} are the integrated emission intensities, and η_r and η_{std} are the refractive indices of the solvents.[4] For all measurements, the same slit widths for excitation and emission were maintained. Time-correlated single photon counting (TCSPC) measurements were carried out for recording of the luminescence decay[5] profile for the tridentate ligand HL^{SBz} and Ir(III) complexes in dichloromethane solution using a picosecond diode laser (IBH Nanoled-07) in an IBH Fluorocube apparatus. Air-equilibrated solutions were used for recording of the luminescence lifetime. The fluorescence decays were collected on a Hamamatsu MCP photomultiplier (R3809). The fluorescence decays were analyzed using IBH DAS6 software. GC analysis of the solution was performed on a Perkin Elmer Clarus 600 gas chromatograph equipped with a 30 m (0.25 mm i.d., 0.25 μm film thickness) Elite 5 MS column. Carrier gas He, T1 = 40 °C, initial isotherm time = 2 min, heating rate = 8, T_{final} = 300 °C, final isotherm time = 5, flow = 1ml/min. The mass spectrometry data were collected after electron ionization at 70 eV. Electrochemical measurements were carried out at 27 °C with VersaStat II Princeton Applied Research potentiostat/galvanostat under argon atmosphere. The cell contained a Pt working electrode and a Pt wire auxiliary electrode. Tetraethylammnium perclorate (NEt_4ClO_4) was used as a supporting electrolyte and the potentials are referrenced to the Ag/AgCl electrode without junction correction. Coulometric

oxidation was performed at a constant potential of 1.0 V vs Ag/AgCl at 300 K in 1:1 CH_2Cl_2:CH_3CN in the presence of NEt_4ClO_4 under argon. Electron paramagnetic resonance (EPR) spectra were recorded in standard quartz EPR tubes using JEOL JES-FA200 X-band spectrometer.

Crystallographic Studies. X-ray intensity data for all the representative compounds were measured at 296 (2) K on Bruker AXS SMART APEX II equipped with a CCD diffractometer using graphite-monochromator (Mo Kα, λ = 0.71073 Å). Metal atoms were located by direct methods, and the rest of the non-hydrogen atoms emerged from successive Fourier synthesis. The structures were refined by full-matrix least squares procedures on F^2. All non-hydrogen atoms of were refined anisotropically except that of **5b.** Metal atoms were located and solved by direct methods using the program SHELXS-97.[6] The refinement and all further calculations were carried out using SHELXL-97.[7] The H-atoms were included in calculated positions and treated as riding atoms using SHELXL default parameters. Calculations were performed using the SHELXTL v 6.14 program package.[8] Thermal ellipsoids are drawn at the 40% probability level. Molecular structure plots were drawn using the Oak Ridge thermal ellipsoid plot ORTEP.[9] For compound **4**, electron density map showed the presence of some unassignable peaks, which were removed by running the program SQUEEZE.[10] For complex **5b**, all atoms are refined anisotropically except C12, C25, C43 and C45. Attempts to obtain a better data set are impeded by the poor crystal quality. Some of the carbon atoms of PPh_3 are found to be refined with higher ADP probably due to poor and highly overlapping X-ray diffraction data. However, the connectivity and other broad structural features of the main complex are refined to a reasonable degree with respect to data quality and are undoubtedly correct. The final least-squares refinement ($I > 2.00\sigma(I)$) converged to reasonably good R values (ESI, Table S1†).

Computational Details.

The molecular geometry of the singlet ground state (S_0) and the first excited triplet state (T_1) of the synthesized complexes **2a**, **3** and **4** have been calculated by DFT method using the (R)B3LYP[11] hybrid functional approach incorporated in GAUSSIAN 09 program package.[12] The geometries of the complexes were fully optimized in gas phase without imposing any symmetry constraints and ligand simplification. The nature of all the stationary points was checked by computing vibrational frequencies, and all the species were found to be true potential energy minima, as no imaginary frequency were obtained (NImag = 0). The single crystal X-ray coordinates have been used as the initial input in all calculations for **2a**, **3** and **4**. The calculated S_0 structures nicely correspond to the geometrical parameters obtained experimentally by X-ray diffractometry. On the basis of the optimized ground and excited state geometries, the absorption and emission spectral properties in dichloromethane (CH_2Cl_2) media were

calculated by the time-dependent density functional theory (TD-DFT)[13] approach associated with the conductor-like polarizable continuum model (CPCM).[14] We computed the lowest 100 singlet–singlet transitions and 100 singlet–triplet transitions in absorption and emission processes respectively and the results of the TD calculations were qualitatively similar to the observed spectra. The TD-DFT approach is now well-known as a rigorous formalism for the treatment of electronic excitation energies within the DFT framework for calculating spectral properties of many transition metal complexes.[15] Hence TD-DFT had been shown to provide a reasonable spectral feature for the compounds under investigation. The iridium atom was described by a double-ζ basis set with the effective core potential of Hay and Wadt (LANL2DZ)[16] and the 6-31G basis set[17] was used for the other elements present in the complexes to optimize both the ground state and the lowest lying triplet excited state geometries. The calculated electronic density plots for frontier molecular orbitals were prepared by using the GaussView 5.0 software. GaussSum program, version 2.2[18] was used to calculate the molecular orbital contributions from groups or atoms.

References

(1) B. P. Sullivan, D. J. Salmon, T. J. Meyer and J. Peedrin, *Inorg. Chem*., 1979, **18**, 3369–3374.

(2) J. V. Houten and R. J. Watts, *J. Am. Chem. Soc*., 1976, **98**, 4853–4858.

(3) (a) W. H. Melhuish, *J. Phys. chem*., 1961, **65**, 229–235; (b) W. R. Dawson and M. W. Windsor, *J. Phys. Chem*., 1968, **72**, 325–3260 and references therein.

(4) (a) F. I. El-Dossoki, *J. Chin. Chem. Soc*., 2007, **54**, 1129–1137; (b) P. Pacak, *Chem. Papers*., 1991, **45**, 227–232; (c) R. A. MacRae, E.T. Arakawa and M. W. Williams, *Journal of Chemical and Engineering Data,* 1978, **23**, 189–190.

(5) (a) D. F. Eatond, *Pure & Appl. Chem*., 1990, **62**, 1631–1648; (b) W. R. Ware, L. J. Doemeny and T. L. Nemzek, *J. Phys. Chem*., 1973, **77**, 2038–2048.

(6) G. M. Sheldrick, *SHELXS-97*, *Program for Crystal Structure Solution*; University of Göttingen: Göttingen, Germany, 1997.

(7) G. M. Sheldrick, *SHELXL-97*, *Program for Refining X-ray Crystal Structures*; University of Göttingen: Göttingen, Germany, 1997.

(8) G. M. Sheldrick, SHELXTL *v*. 6.14, Bruker AXS Inc., Madison, WI, 2003.

(9) C. K. Johnson, *ORTEP*; Report ORNL-5138; Oak Ridge National Laboratory: Oak Ridge, TN, 1976.

(10) A. L. Spek, *PLATON*. *J. Appl. Crystallogr*., 2003, **36**, 7–13.

(11) (a) A. D. Becke, *J. Chem. Phys*., 1993, **98**, 5648–5652; (b) C. Lee, W. Yang, R. G. Parr, *Phys. Rev. B*, 1988, **37**, 785–789.

(12) Gaussian 09, Revision A.01, M. J. Frisch, G. W. Trucks, H. B. Schlegel, G. E. Scuseria, M. A. Robb, J. R. Cheeseman, G. Scalmani, V. Barone, B. Mennucci, G. A. Petersson, H. Nakatsuji, M. Caricato, X. Li, H. P. Hratchian, A. F. Izmaylov, J. Bloino, G. Zheng, J. L. Sonnenberg, M. Hada, M. Ehara, K. Toyota, R. Fukuda, J. Hasegawa, M. Ishida, T. Nakajima, Y. Honda, O. Kitao, H. Nakai, T. Vreven, J. A. Montgomery, Jr., J. E. Peralta, F. Ogliaro, M. Bearpark, J. J. Heyd, E. Brothers, K. N. Kudin, V. N. Staroverov, R. Kobayashi, J. Normand, K. Raghavachari, A. Rendell, J. C. Burant, S. S. Iyengar, J. Tomasi, M. Cossi, N. Rega, J. M. Millam, M. Klene, J. E. Knox, J. B. Cross, V. Bakken, C. Adamo, J. Jaramillo, R. Gomperts, R. E. Stratmann, O. Yazyev, A. J. Austin, R. Cammi, C. Pomelli, J. W. Ochterski, R. L. Martin, K. Morokuma, V. G. Zakrzewski, G. A. Voth, P. Salvador, J. J. Dannenberg, S. Dapprich, A. D. Daniels, O. Farkas, J. B. Foresman, J. V. Ortiz, J. Cioslowski and D. J. Fox, Gaussian, Inc., Wallingford CT, 2009.

(13) (a) J. Autschbach, T. Ziegler, S. J. A. Gisbergen and E. J. Baerends, *J. Chem. Phys.*, 2002, **116**, 6930–6940; (b) K. L. Bak, P. Jørgensen, T. Helgaker, K. Rund and H. J. A. Jenson, *J. Chem. Phys.*, 1993, **98**, 8873–8887; (c) T. Helgaker and P. Jørgensen, *J. Chem. Phys.*, 1991, **95**, 2595–2601; (d) E. K. U. Gross and W. Kohn, *Adv. Quantum Chem.*, 1990, **21**, 255–291.

(14) (a) M. Cossi, N. Rega, G. Scalmani and V. Barone, *J. Comput. Chem.*, 2003, **24**, 669–681; (b) M. Cossi and V. Barone, *J. Chem. Phys.*, 2001, **115**, 4708–4717; (c) V. Barone and M. Cossi, *J. Phys. Chem. A*, 1998, **102**, 1995–2001.

(15) (a) T. Liu, H. X. Zhang and B. H. Xia, *J. Phys. Chem. A*, 2007, **111**, 8724–8730; (b) A. Albertino, C. Garino, S. Ghiani, R. Gobetto, C. Nervi, L. Salassa, E. Rosenverg, A. Sharmin, G. Viscardi, R. Buscaino, G. Cross and M. Milanesio, *J. Organomet. Chem.*, 2007, **692**, 1377–1391; (c) X. Zhou, H. X. Zhang, Q. J. Pan, B. H. Xia and A. C. Tang, *J. Phys. Chem. A*, 2005, **109**, 8809–8818; (d) X. Zhou, A. M. Ren and J. K. Feng, *J. Organomet. Chem.*, 2005, **690**, 338–347.

(16) (a) P. J. Hay and W. R. Wadt, *J. Chem. Phys.*, 1985, **82**, 299–310; (b) P. J. Hay and W. R. Wadt, *J. Chem. Phys.*, 1985, **82**, 270–283.

(17) (a) M. S. Gordon, J. S. Binkley, J. A. Pople, W. J. Pietro and W. J. Hehre, *J. Am. Chem. Soc.*, 1982, **104**, 2797–2803; (b) J. S. Binkley, J. A. Pople and W. J. Hehre, *J. Am. Chem. Soc.*, 1980, **102**, 939–947.

(18) N. M. O'Boyle, A. L. Tenderholt and K. M. Langner, *J. Comp. Chem.*, 2008, **29**, 839–845.

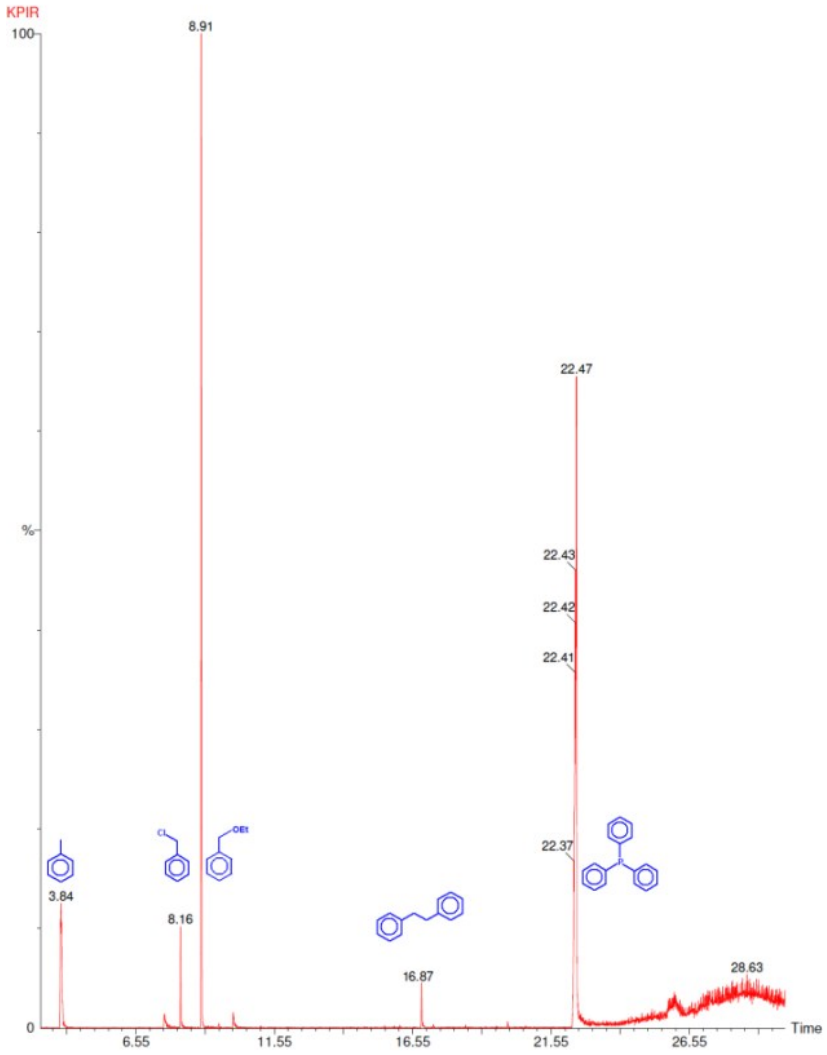

Fig. S1 Selected ion monitoring GC-MS study the typical reaction mixture. Relative area ratio of toluene, benzyl chloride, ethyl benzyl ether and bibenzyl is 11:5:13:1. Retention time is given in minute.

Table S1 Summarized Crystallographic Data for **2a**, **3**, **4** and **5b**

Crystallographic Parameter	2a	3.2CH_2Cl_2	4.CH_2Cl_2	5b
Empirical formula	$C_{37}H_{30}Cl_2IrN_2PS$	$C_{48}H_{38}ClIrN_2P_2S$, $2CH_2Cl_2$	$C_{48}H_{38}ClIrN_2O_2P_2S$, CH_2Cl_2	$C_{33}H_{28}BrClIrN_2PS$
fw	828.76	1134.31	1081.38	823.17
T/K	296(2)	296(2)	296(2)	296(2)
Cryst syst	triclinic	Orthorhombic	Orthorhombic	Monoclinic
Space group	$P\bar{1}$	$Cmc2_1$	$Cmc2_1$	$P2_1$
a/Å	9.622(1)	14.995(10)	15.375(2)	10.072(1)
b/Å	11.146(1)	18.277(12)	18.420(2)	25.822(3)
c/Å	16.484(2)	17.452(11)	17.336(2)	11.786(1)
α /deg	92.508(2)	90	90	90
β /deg	105.399(2)	90	90	102.538(3)
γ/deg	109.514(2)	90	90	90
V/Å^3	1589.4(3)	4783.0(5)	4909.75(10)	2992.1(5)
Z	2	4	4	4
D_c/Mgm^{-3}	1.732	1.575	1.463	1.827
μ/mm^{-1}	4.515	3.218	3.029	6.037
F(000)	816	2256	2152	1600
cryst size/mm^3	0.42×0.33×0.29	0.43×0.38×0.26	0.33×0.22×0.16	0.47×0.25×0.23
θ/deg	1.96- 27.32	1.76-30.00	1.73- 30.53	1.58-27.59
measured reflns	20827	34021	25391	39576
unique reflns/R_{int}	6990/0.0439	7084/0.0447	7289/0.0255	13393/0.0728
GOF on F^2	1.047	1.076	1.022	1.074
R1,[a] wR2[b] [$I > 2\sigma(I)$]	0.0334, 0.0779	0.0262, 0.0627	0.0250, 0.0654	0.0600, 0.1381
R indices (all data) R1,wR2	0.0413, 0.0819	0.0277, 0.0633	0.0291, 0.0665	0.0763, 0.1451

[a] $R1 = \Sigma||F_o| - |F_c||/\Sigma|F_o|$. [b] $wR2 = [\Sigma w(F_o^2 - F_c^2)^2/\Sigma w(F_o^2)^2]^{1/2}$.

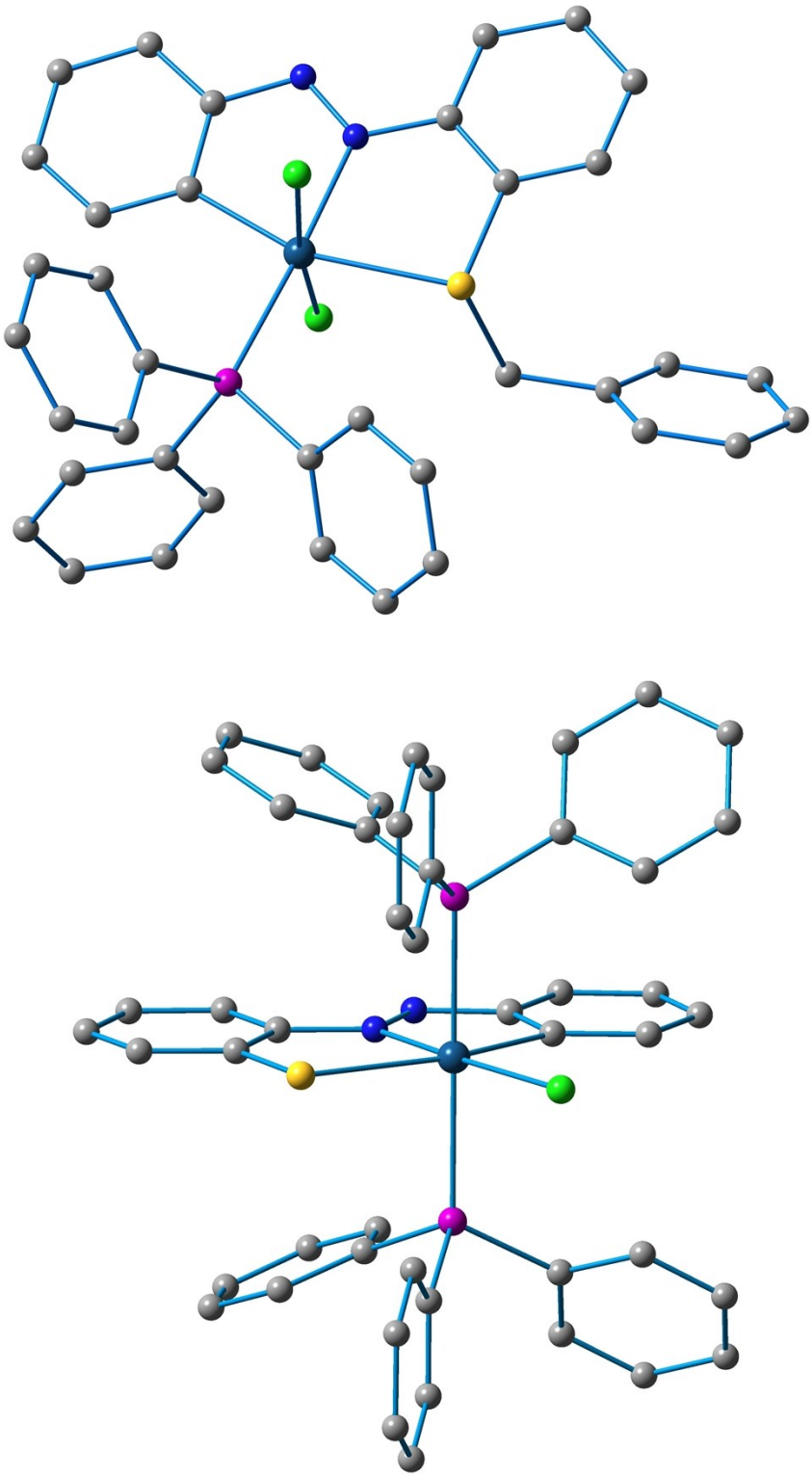

Fig. S2 Optimized molecular structure of **2a** (top) and **3** (bottom) (Ir: metallic blue, N: blue, P: pink, Cl: green, C: grey. Hydrogen atoms are omitted for clarity).

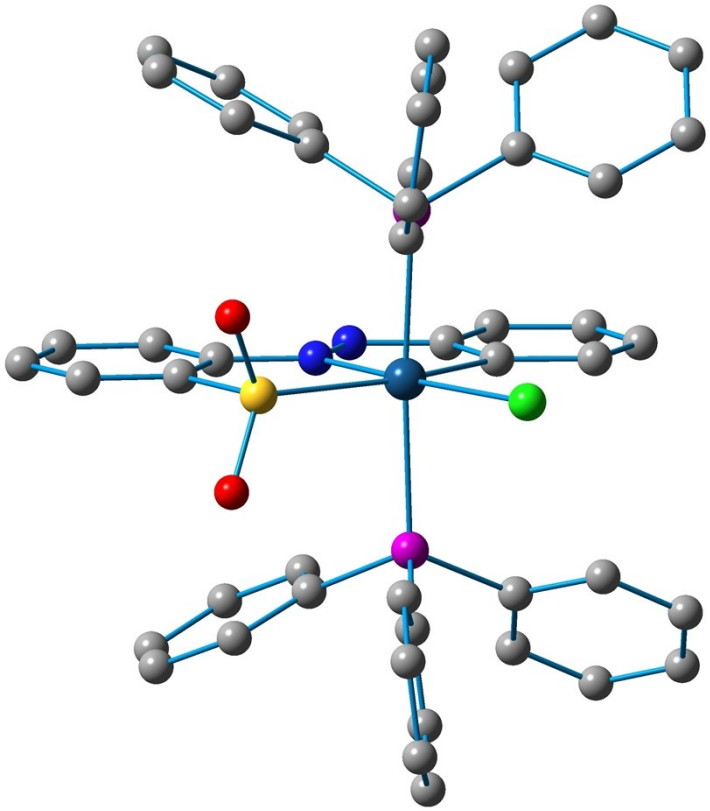

Fig. S3 Optimized molecular structure of **4** (Ir: metallic blue, N: blue, O: red, P: pink, Cl: green, C: grey. Hydrogen atoms are omitted for clarity).

Table S2 Selected optimized geometrical parameters of **2a**, **3** and **4** in the ground and lower lying triplet excited states at B3LYP level

Bond Lengths (Å)								
2a			**3**			**4**		
	S_0	T_1		S_0	T_1		S_0	T_1
Ir1–Cl2	2.43674	2.42623	Ir1–Cl2	2.47547	2.48241	Ir1–P2	2.47028	2.48369
Ir1–Cl3	2.44177	2.42752	Ir1–S3	2.51972	2.47027	Ir1–S3	2.47293	2.50569
Ir1–S4	2.52116	2.54729	Ir1–P4	2.43623	2.44911	Ir1–Cl4	2.45711	2.39911
Ir1–P5	2.38985	2.42187	Ir1–N5	2.02002	2.02135	Ir1–C8	2.05304	2.07444
Ir1–N6	2.04861	2.01799	Ir1–C7	2.05925	2.04221	Ir1–N6	2.03073	2.09430
Ir1–C8	2.02696	2.00814	Ir1–P60	2.43628	2.44911	Ir1–P62	2.47028	2.48369
N6–N7	1.28902	1.40839	N5–N6	1.29938	1.39980	N6–N7	1.29729	1.36248
S4–C28	1.87722	1.87957				S3–O5	1.51796	1.51355
						S3–O61	1.51796	1.51355
Bond Angles (°)								
	S_0	T_1		S_0	T_1		S_0	T_1
Cl2–Ir1–Cl3	172.416	173.798	Cl2–Ir1–S3	101.195	102.610	P2–Ir1–S3	90.379	91.354
Cl2–Ir1–S4	92.285	91.856	Cl2–Ir1–P4	87.815	87.518	P2–Ir1–Cl4	86.911	87.595
Cl2–Ir1–P5	95.873	94.854	Cl2–Ir1–N5	175.652	175.413	P2–Ir1–N6	93.105	92.327
Cl2–Ir1–N6	87.055	88.276	Cl2–Ir1–C7	96.622	95.691	P2–Ir1–C8	90.596	89.661
Cl2–Ir1–C8	86.874	86.870	Cl2–Ir1–P60	87.815	87.518	P2–Ir1–P62	173.790	175.002
Cl3–Ir1–S4	83.567	84.163	S3–Ir1–P4	88.659	89.929	S3–Ir1–Cl4	102.943	107.053
Cl3–Ir1–P5	91.081	90.457	S3–Ir1–N5	83.153	81.977	S3–Ir1–N6	83.378	78.552
Cl3–Ir1–N6	86.114	86.434	S3–Ir1–C7	162.183	161.699	S3–Ir1–C8	161.918	154.972
Cl3–Ir1–C8	95.019	95.399	S3–Ir1–P60	88.659	89.929	S3–Ir1–P62	90.379	91.354
S4–Ir1–P5	99.468	98.695	P4–Ir1–N5	92.316	92.524	Cl4–Ir1–N6	173.679	174.396
S4–Ir1–N6	82.538	81.462	P4–Ir1–C7	92.039	90.870	Cl4–Ir1–C8	95.138	97.976
S4–Ir1–C8	161.334	161.563	P4–Ir1–P60	174.338	174.880	Cl4–Ir1–P62	86.911	87.595
P5–Ir1–N6	176.360	176.857	N5–Ir1–C7	79.030	79.722	N6–Ir1–C8	78.541	76.420
P5–Ir1–C8	99.166	99.740	N5–Ir1–P60	92.316	92.524	N6–Ir1–P62	93.105	92.327
N6–Ir1–C8	78.796	80.117	C7–Ir1–P60	92.039	90.870	C8–Ir1–P62	90.596	89.661

Table S3 Frontier Molecular Orbital Composition (%) in the Ground State for **2a**

Orbital	MO	Energy (EV)	Contribution (%)							Main Bond Type
			Ir	Ligand				PPh_3	Cl	
				Azo	Ph	S	CH_2Ph			
180	L + 5	–0.66	5	0	3	3	1	87	1	$\pi^*(PPh_3)$
179	L + 4	–0.67	2	0	3	1	1	93	1	$\pi^*(PPh_3)$
178	L + 3	–0.81	13	0	10	4	2	65	6	$\pi^*(L) + \pi^*(PPh_3)$
177	L + 2	–0.97	2	1	47	10	31	8	1	$\pi^*(L)$
176	L + 1	–1.21	43	4	2	0	1	23	27	$d_z^2(Ir) + \pi^*(L) + \pi^*(Cl)$
175	L	–2.69	3	46	46	0	0	1	3	$\pi^*(L)$
174	H	–5.56	42	3	24	2	1	1	27	$d_{zx}(Ir) + \pi(L) + \pi(Cl)$
173	H – 1	–5.87	36	2	6	0	0	3	53	$d_{yz}(Ir) + \pi(Cl)$
172	H – 2	–6.26	12	5	37	10	1	4	30	$\pi(L) + \pi(Cl)$
171	H – 3	–6.39	13	5	30	10	16	7	18	$\pi(L) + \pi(Cl)$
170	H – 4	–6.57	1	10	28	1	2	24	34	$\pi(L) + \pi(Cl)$
169	H – 5	–6.61	1	4	46	3	1	19	28	$\pi(L) + \pi(Cl)$
HOMO–LUMO gap = 2.87 eV										

Table S4 Frontier Molecular Orbital Composition (%) in the Ground State for **3**

	MO	Energy (EV)	Contribution (%)						Main Bond Type
			Ir	Ligand			PPh_3	Cl	
				Azo	Ph	S			
216	L + 5	–0.42	2	0	4	0	94	0	$\pi^*(PPh_3)$
215	L + 4	–0.47	4	1	0	1	92	1	$\pi^*(PPh_3)$
214	L + 3	–0.61	0	0	2	0	98	0	$\pi^*(PPh_3)$
213	L + 2	–0.62	0	0	0	0	99	0	$\pi^*(PPh_3)$
212	L + 1	–1.09	25	3	1	1	68	3	$d_z^2(Ir) + \pi^*(PPh_3)$
211	L	–2.30	5	45	43	3	3	0	$\pi^*(L)$
210	H	–4.60	10	4	34	49	3	0	$d_{zx}(Ir) + \pi(L) + \pi(S)$
209	H – 1	–5.42	36	0	14	26	2	22	$d_{xy}(Ir) + \pi(L) + \pi(S) + \pi(Cl)$
208	H – 2	–5.83	16	4	37	4	17	22	$d_{zx}(Ir) + \pi(L) + \pi(PPh_3) + \pi(Cl)$
207	H – 3	–6.06	19	4	60	0	12	5	$d_{yz}(Ir) + \pi(L) + \pi(PPh_3)$
206	H – 4	–6.18	3	3	47	2	23	21	$\pi(L) + \pi(PPh_3) + \pi(Cl)$
205	H – 5	–6.43	12	1	9	0	74	5	$d(Ir) + \pi(PPh_3)$
HOMO–LUMO gap = 2.30 eV									

Table S5 Frontier Molecular Orbital Composition (%) in the Ground State for **4**

Orbital	MO	Energy (EV)	Contribution (%)						Main Bond Type
			Ir	Ligand			PPh_3	Cl	
				Azo	Ph	SO_2			
224	L + 5	–0.58	5	1	0	0	91	3	$\pi^*(PPh_3)$
223	L + 4	–0.63	0	0	13	0	87	0	$\pi^*(L) + \pi^*(PPh_3)$
222	L + 3	–0.67	1	0	27	2	69	0	$\pi^*(L) + \pi^*(PPh_3)$
221	L + 2	–0.67	8	1	1	2	86	2	$\pi^*(PPh_3)$
220	L + 1	–1.49	30	3	1	1	62	4	$d_z^2(Ir) + \pi^*(PPh_3)$
219	L	–2.81	5	47	43	1	3	0	$\pi^*(L)$
218	H	–5.57	18	0	21	48	1	11	$d_{xy}(Ir) + \pi(L) + \pi(Cl)$
217	H – 1	–6.01	17	6	39	17	11	11	$d_{zx}(Ir) + \pi(L) + \pi(Cl) + \pi(PPh_3)$
216	H – 2	–6.26	8	0	6	9	51	27	$\pi(L) + \pi(PPh_3) + \pi(Cl)$
215	H – 3	–6.34	1	2	21	24	50	2	$\pi(L) + \pi(PPh_3)$
214	H – 4	–6.37	18	0	6	11	39	26	$d_{xy}(Ir) + \pi(L) + \pi(Cl) + \pi(PPh_3)$
213	H – 5	–6.41	12	3	46	1	37	0	$d_{yz}(Ir) + \pi(L)$
HOMO–LUMO gap = 2.76 eV									

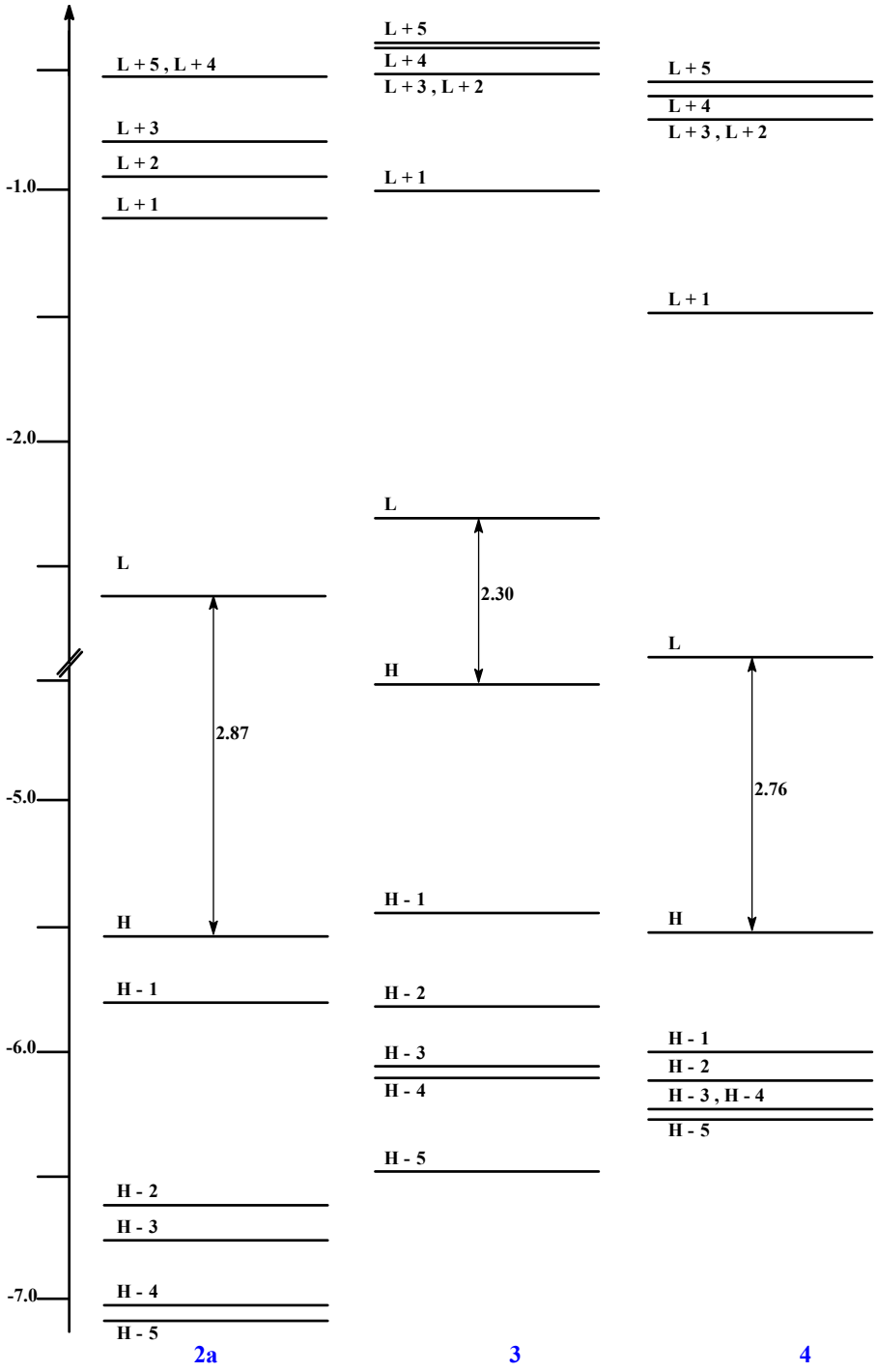

Fig. S4 Partial molecular orbital diagram for complexes **2a**, **3** and **4**. The arrows are intended to highlight the HOMO−LUMO energy gaps. All energy values are given in eV.

Table S6 Orbital composition (%) of HOMO in the ground state for **3** and $\mathbf{3}^{\bullet+}$ and their rhodium analogues at the B3LYP/(6-31G + LANL2DZ) level

Compound	Energy	M	S	Ph	Azo	PPh_3	Cl
$[Ir^{III}(L^S)Cl(PPh_3)_2]$ **3**	–4.60	10	49	34	4	3	0
$[Ir^{III}(L^S)Cl(PPh_3)_2]^+$ $\mathbf{3}^{\bullet+}$	–8.59	15	24	43	5	13	0
$[Rh^{III}(L^S)Cl(PPh_3)_2]$	–4.69	6	51	34	5	4	0
$[Rh^{III}(L^S)Cl(PPh_3)_2]^+$	–8.50	7	13	18	2	54	6

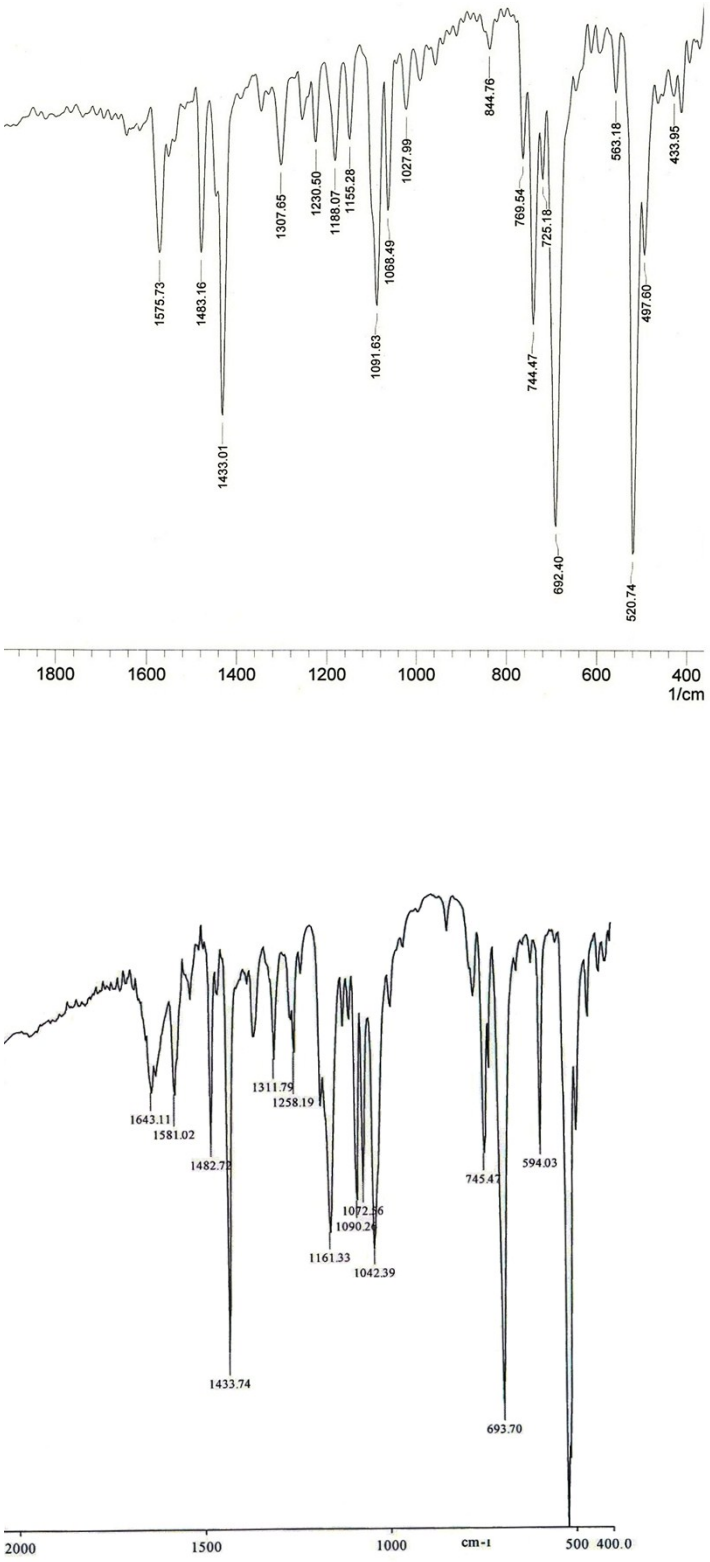

Fig. S5 Experimental Infrared spectra of **3** (top) and **4** (bottom).

Table S7 Predicted Frequencies and IR Intensities Associated with the Stretching Modes of the NN, IrP and SO Chemical Functions in the Optimized Structure from the DFT-B3LYP Method[a]

Modes	frequency transition v cm^{-1} (I_{IR} km/mol)								
	2a			3			4		
	Exp.	Cal.	Assignment	Exp.	Cal.	Assignment	Exp.	Cal.	Assignment
N=N	1433	1418.6 (121.0)	ν_{NN}	1433	1375.09 (26.5)	ν_{NN}	1434	1400.4(32.6)	ν_{NN}
P–Ir–P	693 518	553.1 (119.3) 476.2 (14.2)	ν_{IrP} ρ_{IrP}	692 520	552.56(32.7) 544.04(224.1) 524.43(59.9) 481.42(23.9) 443.95(13.2) 433.62(25.5)	ν_{IrP} sym ν_{IrP} assym σ_{PIrP} σ_{PIrP} ν_{IrP} sym ν_{IrP} assym	694 520	545.1(219.8) 522.7(59.3) 481.1(10.3)	ν_{IrP} asym σ_{PIrP} σ_{PIrP}
O=S=O							1161 1042 – –	1103.0 (250.2) 977.6 (77.0) 975.0(63.5) 544.4(54.2) 494.9 (39.6)	ν_{SO} asym ν_{SO} sym ν_{SO} sym $\sigma_{OSO} + \omega_{OSO}$ σ_{OSO}

[a] ν = stretching mode, σ = scissoring mode, ω = wagging mode, ρ = rocking mode.

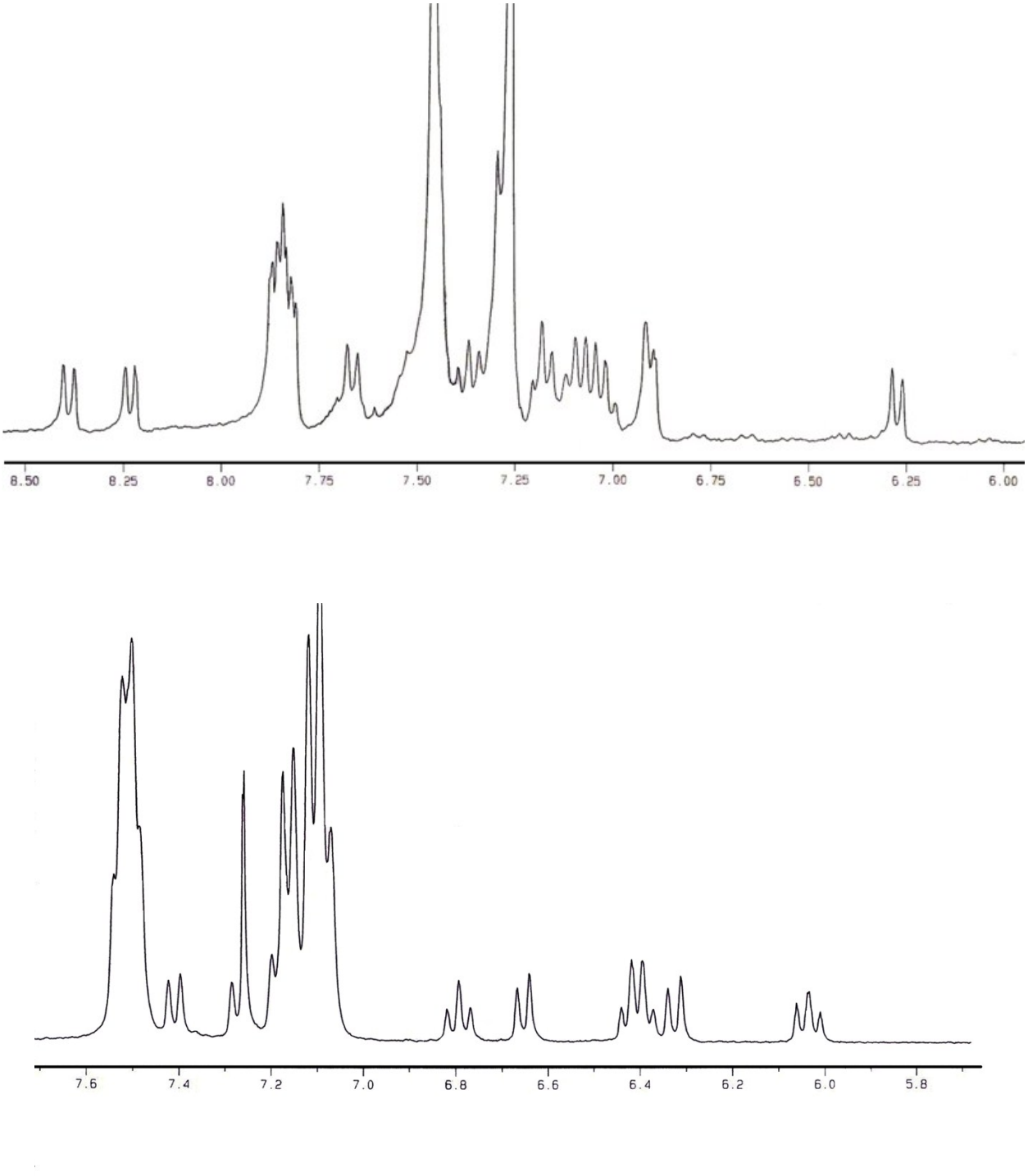

Fig. S6 Relevant section of the ^{1}H NMR spectra of **2a** (top) and **3** (bottom).

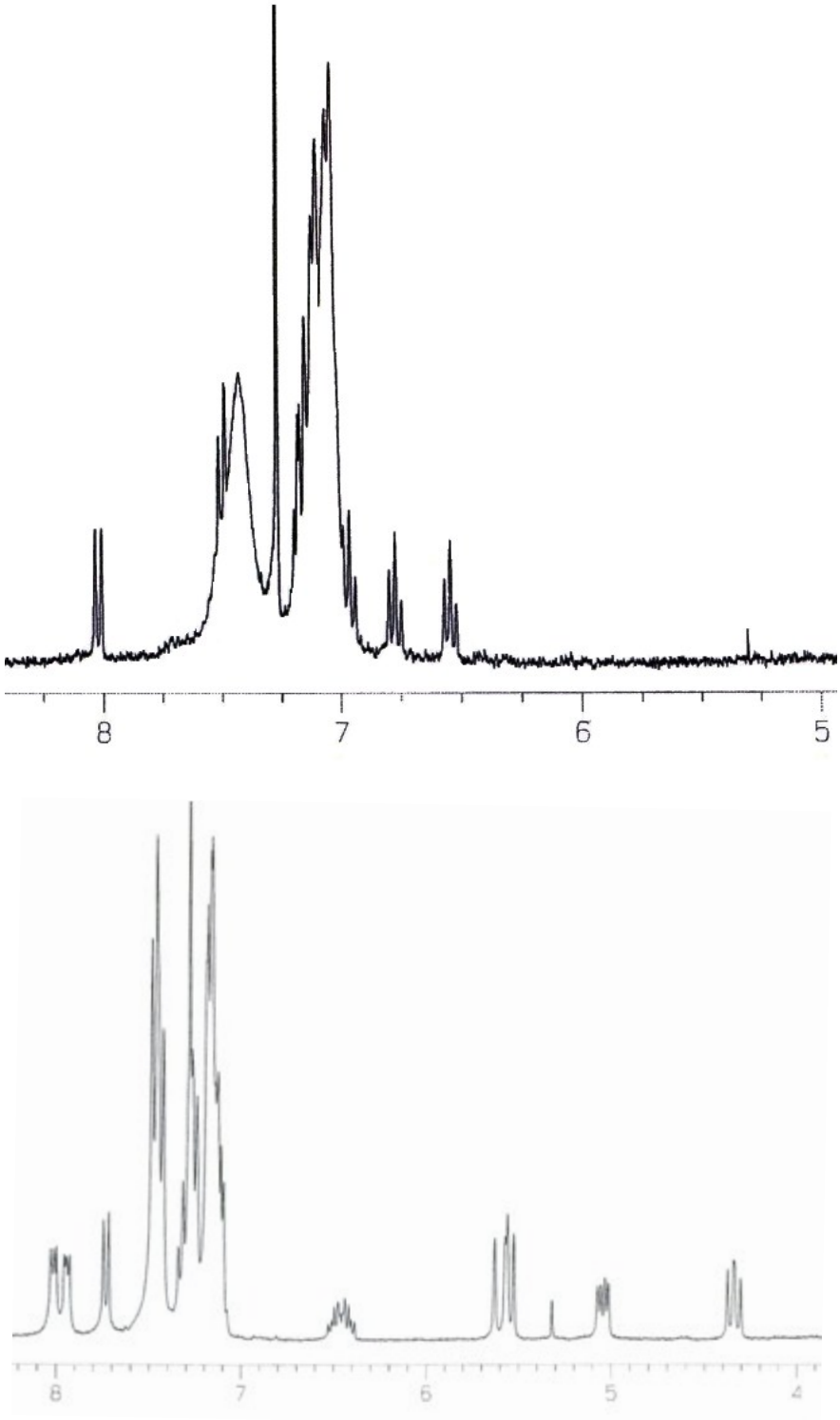

Fig. S7 Relevant section of the ^{1}H NMR spectra of **4** (top) and **5b** (bottom).

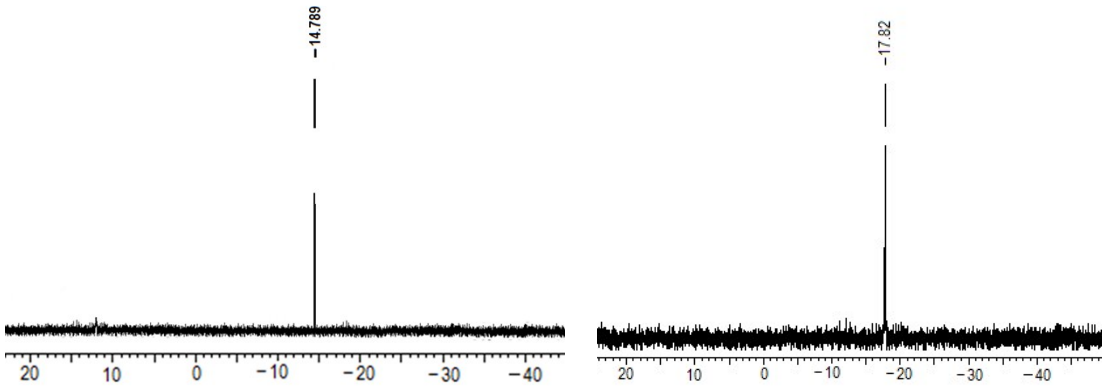

Fig. S8 Relevant section of the ^{31}P NMR spectra of **3** (top left) and **4** (top right).

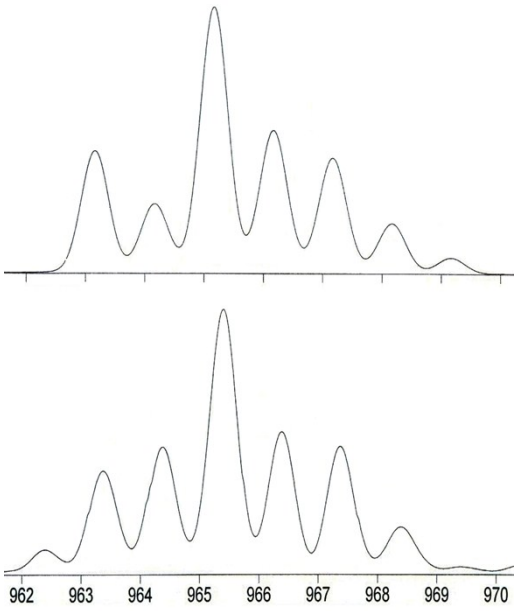

Fig. S9 High-resolution mass spectra of thiolato compounds: simulated isotropic spectrum for $C_{48}H_{38}ClN_2P_2IrS$ *m/z* 965.1641 (top), observed spectrum of **3** (molecular ion peak *m/z* 965.2823) [M^+; 100%] (bottom).

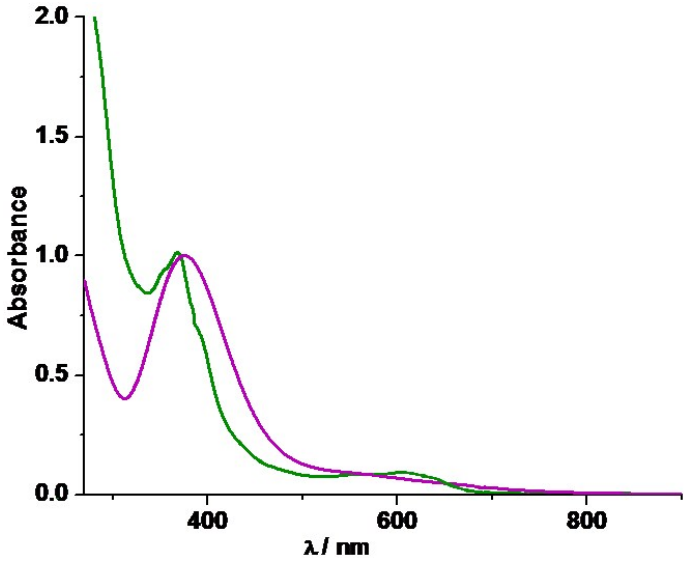

Fig. S10 Experimental (green) and theoretical (violet) absorption spectra of **2a** in dichloromethane.

Table S8 Main optical transition at the TD-DFT/B3LYP/6-31G+LANL2DZ Level for the complex **2a** with composition in terms of molecular orbital contribution of the transition, Computed Vertical excitation energies, and oscillator strength in dichloromethane

	Composition	E (ev)	Oscillator strength (*f*)	λ_{theo} (nm)	Assignment	λ_{exp}[nm] (ε [$M^{-1}cm^{-1}$])
1.	H → L (97%)	2.1551	0.0303	575.29	MLCT/LLCT	630 (1600)
2.	H – 1 → L (93%)	2.6556	0.0254	466.88	MLCT/LLCT	
3.	H – 4 → L (57%) H – 3 → L (15%)	3.0684	0.0336	404.07	LLCT/ILCT	390 (sh) (12000)
4.	H – 3 → L (64%) H – 4 → L (12%)	3.1465	0.1853	394.03	LLCT/ILCT/MLCT	
5.	H – 5 → L (53%)	3.3079	0.0988	374.82	LLCT/ILCT	
6.	H – 5 → L (10%) H – 6 → L (72%)	3.4196	0.0766	362.57	LLCT	
7.	H – 9 → L (32%) H – 7 → L (22%) H – 10 → L (16%)	3.5038	0.0505	353.86	LLCT/ILCT	367 (17000)
8.	H – 7 → L (55%) H – 10 → L (19%) H – 9 → L (16%)	3.5784	0.0239	346.48	LLCT/ILCT	
9.	H – 10 → L (50%) H – 9 → L (41%)	3.6063	0.0305	343.80	LLCT/ILCT	
10.	H – 2 → L + 1 (69%)	3.7660	0.0219	329.22	LMCT	

Table S9 Main optical transition at the TD-DFT/B3LYP/6-31G+LANL2DZ Level for the complex **3** with composition in terms of molecular orbital contribution of the transition, Computed Vertical excitation energies, and oscillator strength in dichloromethane

	Composition	E (eV)	Oscillator strength (f)	λ_{theo} (nm)	Assignment	λ_{exp}[nm] (ε [$M^{-1}cm^{-1}$])
1.	H → L (98%)	1.7253	0.0562	718.61	ILCT/MLCT	733 (2800)
2.	H – 3 → L (80%) H – 4 → L (13%)	3.2010	0.0937	387.32	LLCT/ ILCT	390 (sh) (6400)
3.	H – 4 → L (80%)	3.3034	0.0540	375.32	LLCT	368 (11000), 350 (10000)
4.	H – 5 → L (68%) H – 7 → L (12%)	3.4786	0.1638	356.42	LLCT	
5.	H – 2 → L + 1 (48%) H – 3 → L + 1 (15%) H – 5 → L + 1 (10%)	3.8324	0.0352	323.51	LLCT	
6.	H → L + 9 (62%) H – 2 → L + 1 (12%) H – 3 → L + 1 (10%)	4.1797	0.0453	296.63	LLCT	278 (20000)
7.	H – 16 → L (64%)	4.2270	0.0316	293.31	LLCT/MLCT	
8.	H – 16 → L (24%) H – 1 → L + 4 (21%) H – 1 → L + 7 (13%) H – 1 → L + 10 (10%)	4.2326	0.1177	292.93	LLCT/MLCT	

Table S10 Main optical transition at the TD-DFT/B3LYP/6-31G+LANL2DZ Level for the complex **4** with composition in terms of molecular orbital contribution of the transition, Computed Vertical excitation energies, and oscillator strength in dichloromethane

	Composition	E (ev)	Oscillator strength (*f*)	λ_{theo} (nm)	Assignment	λ_{exp}[nm] (ε [$M^{-1}cm^{-1}$])
1.	H – 3 → L (73%) H – 4 → L (19%)	3.0422	0.0839	407.55	LLCT/ILCT	390 (sh) (17000)
2.	H – 4 → L (73%) H – 3 → L (19%)	3.1518	0.1184	393.37	LLCT/MLCT	
3.	H – 7 → L (76%) H – 8 → L (11%)	3.2736	0.0444	378.74	LLCT	
4.	H – 11 → L (82%) H – 14 → L (12%)	3.5104	0.0269	353.19	ILCT	370 (18000)
5.	H – 14 → L (79%) H – 11 → L (13%)	3.5830	0.1120	346.04	ILCT	
6.	H – 2 → L + 1 (75%) H – 3 → L + 1 (21%)	4.1691	0.5421	297.39	LMCT/LLCT	270 (28000)
7.	H – 4 → L + 1 (64%) H – 3 → L + 1 (20%)	4.2836	0.0744	289.44	LMCT/LLCT	

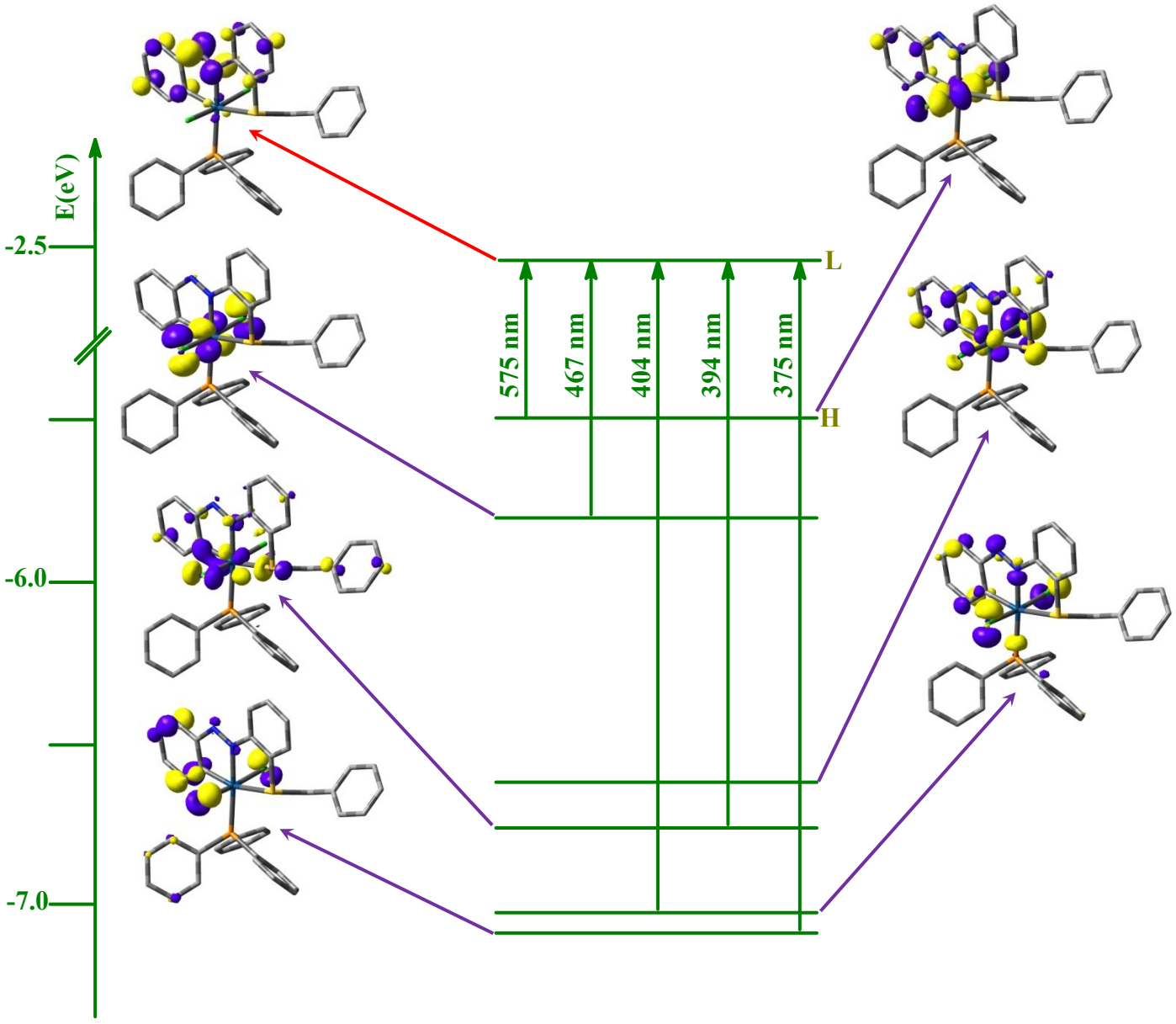

Fig. S11 Partial molecular orbital diagram related to the absorption of complex **2a** with some selected FMOs mainly involved in the electronic transitions

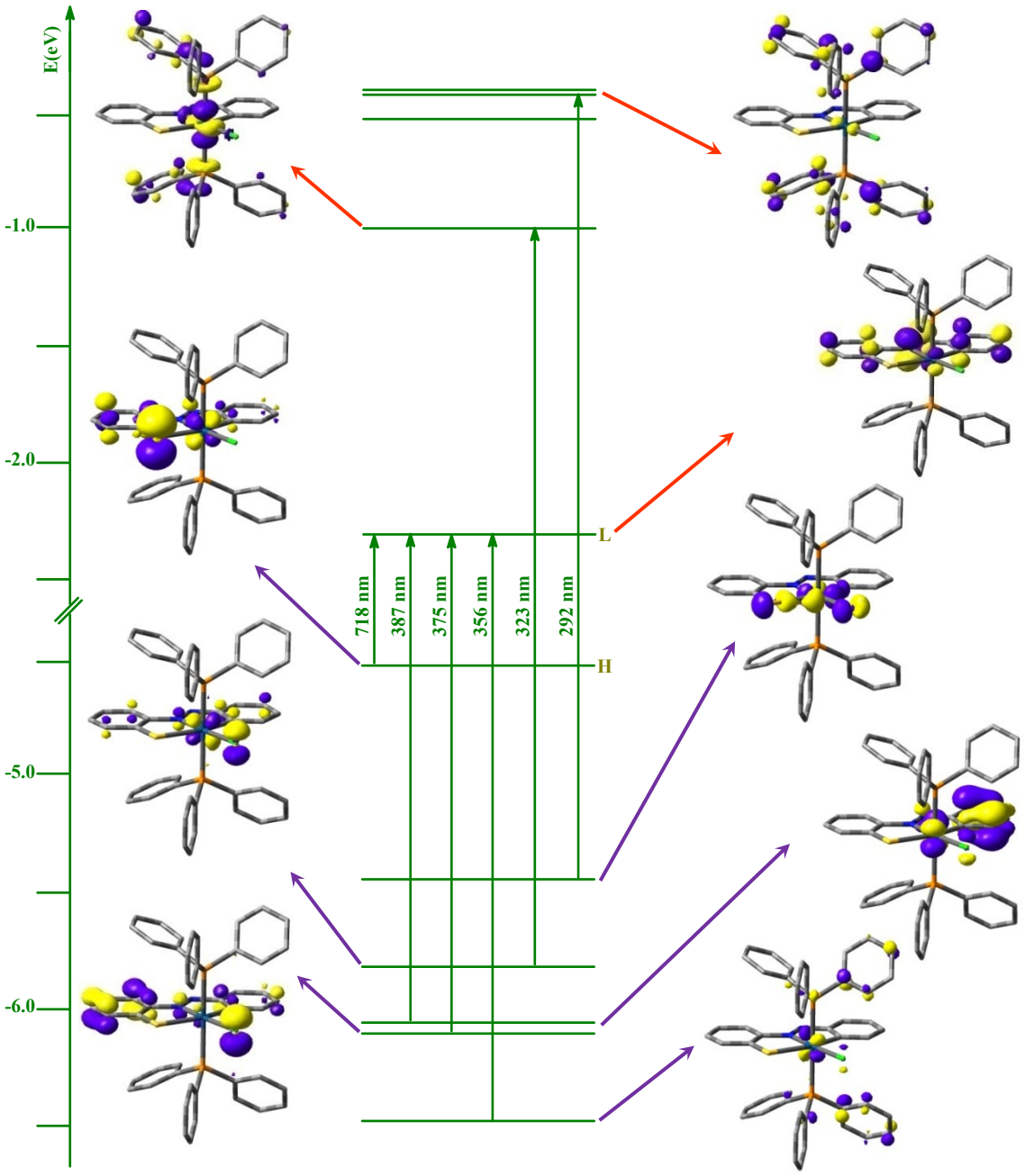

Fig. S12 Partial molecular orbital diagram related to the absorption of complex **3** with some selected FMOs mainly involved in the electronic transitions.

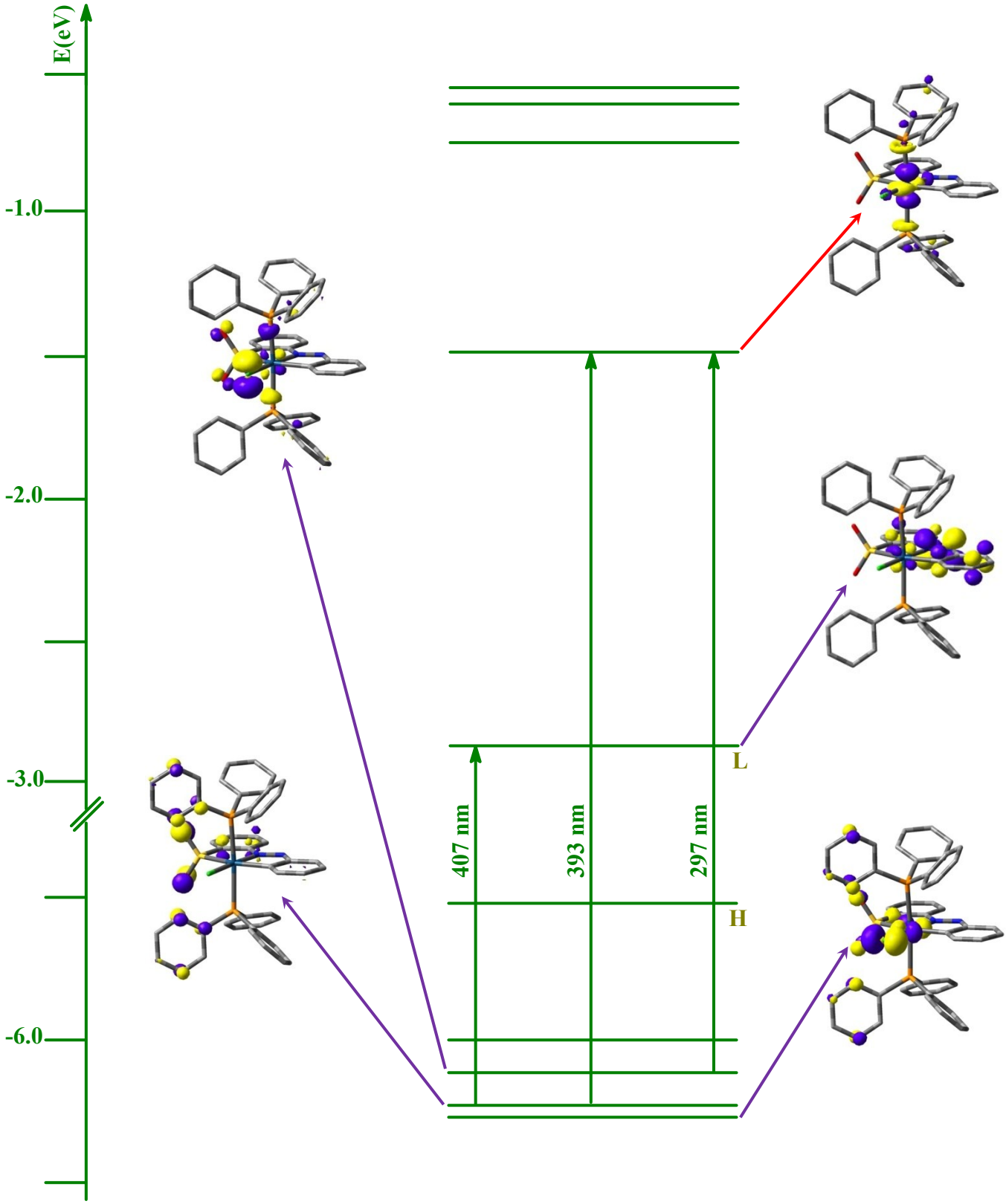

Fig. S13 Partial molecular orbital diagram related to the absorption of complex **4** with some selected FMOs mainly involved in the electronic transitions

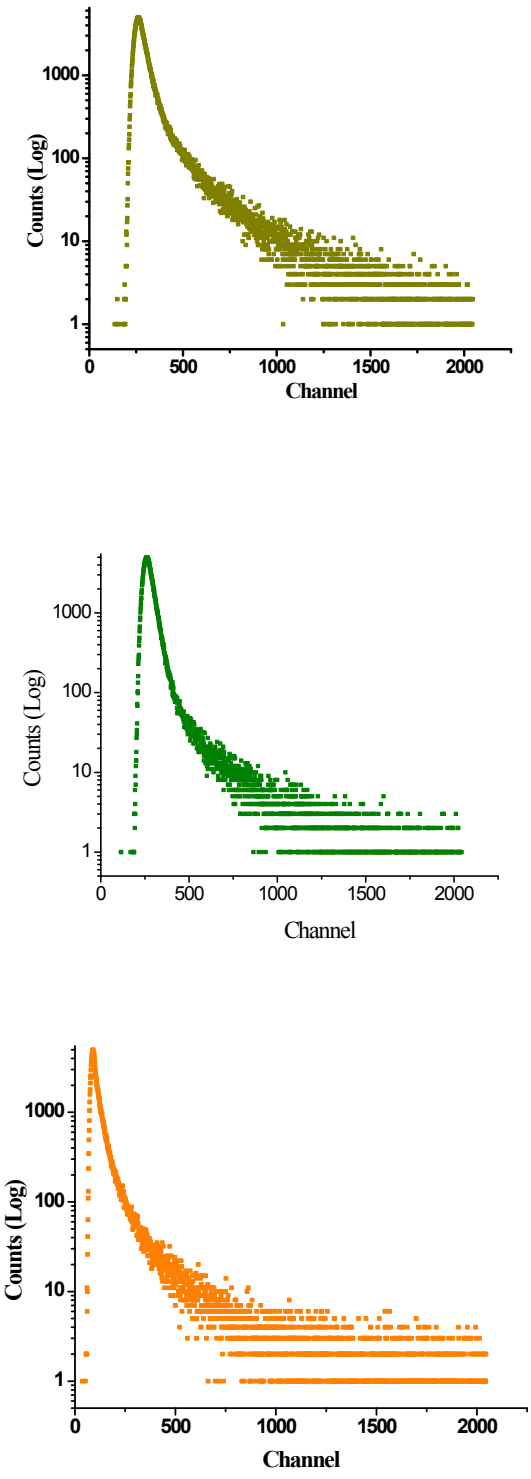

Fig. S14 Changes in the time-resolved photoluminescence decay of complexes **2a** (top), **3** (middle) and **4** (bottom) in dichloromethane at room temperature obtained with 330 nm excitation. The emission at 442, 439 and 400 nm was monitored.

Table S11 Frontier Molecular Orbital Composition (%) in the Excited State for **2a**

Orbital	α–MO	Energy (EV)	Contribution (%)							Main Bond Type
			Ir	Ligand				PPh_3	Cl	
				Azo	Ph	S	CH_2Ph			
181	L + 5	–0.51	1	0	4	1	1	92	0	$\pi^*(PPh_3)$
180	L + 4	–0.75	4	0	3	2	1	90	1	$\pi^*(PPh_3)$
179	L + 3	–0.76	2	0	4	1	1	91	1	$\pi^*(PPh_3)$
178	L + 2	–0.90	7	0	24	8	15	42	3	$\pi^*(L) + \pi^*(PPh_3)$
177	L + 1	–0.99	7	1	24	7	24	36	1	$\pi^*(L) + \pi^*(PPh_3)$
176	L	–1.44	45	3	3	1	1	16	31	$d_z^2(Ir) + \pi^*(Cl)$
175	H	–4.38	5	43	48	0	0	1	3	$\pi(L)$
174	H – 1	–5.83	31	7	37	4	2	1	19	$d_{yz}(Ir) + \pi(L) + \pi(Cl)$
173	H – 2	–6.10	31	3	12	0	0	3	51	$d_{yz}(Ir) + \pi(L) + \pi(Cl)$
172	H – 3	–6.37	11	6	32	5	1	5	40	$\pi(L) + \pi(Cl)$
171	H – 4	–6.52	11	2	25	15	22	4	20	$\pi(L) + \pi(Cl)$
170	H – 5	–6.64	2	20	10	0	0	41	27	$\pi(L) + \pi(PPh_3) + \pi(Cl)$

Orbital	β–MO	Energy (EV)	Contribution (%)							Main Bond Type
			Ir	Ligand				PPh_3	Cl	
				Azo	Ph	S	CH_2Ph			
179	L + 5	–0.75	1	0	4	2	4	88	1	$\pi^*(PPh_3)$
178	L + 4	–0.86	5	0	19	9	23	40	3	$\pi^*(L) + \pi^*(PPh_3)$
177	L + 3	–0.94	7	1	15	5	21	49	2	$\pi^*(L) + \pi^*(PPh_3)$
176	L + 2	–1.34	44	4	3	1	1	18	30	$d_z^2(Ir) + \pi^*(PPh_3) + \pi^*(Cl)$
175	L + 1	–2.08	1	37	57	0	1	1	3	$\pi^*(L)$
174	L	–4.16	22	20	50	2	1	1	5	$d_{zx}(Ir) + \pi^*(L)$
173	H	–5.80	31	6	31	0	0	1	31	$d_{zx}(Ir) + \pi(L) + \pi(Cl)$
172	H – 1	–5.99	32	2	9	1	0	4	52	$d_{yz}(Ir) + \pi(Cl)$
171	H – 2	–6.42	14	1	28	15	10	3	30	$\pi(L) + \pi(Cl)$
170	H – 3	–6.51	3	22	20	3	2	27	23	$\pi(L) + \pi(PPh_3) + \pi(Cl)$
169	H – 4	–6.54	5	9	39	8	4	13	22	$\pi(L) + \pi(Cl)$
168	H – 5	–6.81	5	0	17	8	19	32	20	$\pi(L) + \pi(PPh_3) + \pi(Cl)$

Table S12 Frontier Molecular Orbital Composition (%) in the Excited State for **3**

Orbital	α–MO	Energy (EV)	Contribution (%)						Main Bond Type
			Ir	Ligand			PPh_3	Cl	
				Azo	Ph	S			
217	L + 5	–0.29	1	0	7	0	92	0	$\pi^*(PPh_3)$
216	L + 4	–0.47	1	0	8	0	90	0	$\pi^*(PPh_3)$
215	L + 3	–0.49	3	0	0	1	95	0	$\pi^*(PPh_3)$
214	L + 2	–0.57	0	0	1	0	99	0	$\pi^*(PPh_3)$
213	L + 1	–0.63	0	0	0	1	99	1	$\pi^*(PPh_3)$
212	L	–1.17	25	3	1	1	68	3	$d_z^2(Ir) + \pi^*(PPh_3)$
211	H	–3.8	6	42	45	3	4	0	$\pi(L)$
210	H – 1	–5.1	16	7	47	27	3	0	$d_{zx}(Ir) + \pi(L) + \pi(S)$
209	H – 2	–5.56	39	0	11	18	2	30	$d_{xy}(Ir) + \pi(Cl) + \pi(S)$
208	H – 3	–5.91	15	4	29	6	15	30	$d_{yz}(Ir) + \pi(L) + \pi(S) + \pi(PPh_3)$
207	H – 4	–6.02	8	3	66	1	20	2	$\pi(L) + \pi(PPh_3)$
206	H – 5	–6.23	2	3	51	7	17	20	$\pi(L) + \pi(Cl) + \pi(PPh_3)$

Orbital	β–MO	Energy (EV)	Contribution (%)						Main Bond Type
			Ir	Ligand			PPh_3	Cl	
				Azo	Ph	S			
215	L + 5	–0.48	3	0	0	1	96	0	$\pi^*(PPh_3)$
214	L + 4	–0.57	0	0	1	0	99	0	$\pi^*(PPh_3)$
213	L + 3	–0.62	0	0	0	1	99	1	$\pi^*(PPh_3)$
212	L + 2	–1.12	24	3	1	1	69	2	$d_z^2(Ir) + \pi^*(PPh_3)$
211	L + 1	–1.68	3	38	54	2	3	0	$\pi^*(L)$
210	L	–3.48	12	12	40	33	3	0	$d_{zx}(Ir) + \pi^*(L) + \pi^*(S)$
209	H	–5.43	10	13	51	18	3	5	$d_{yz}(Ir) + \pi(L) + \pi(S)$
208	H – 1	–5.48	39	0	12	19	2	27	$d_{xy}(Ir) + \pi(L) + \pi(Cl) + \pi(S)$
207	H – 2	–5.75	13	2	71	1	12	1	$d_{yz}(Ir) + \pi(L) + \pi(PPh_3)$
206	H – 3	–6.03	16	1	18	1	18	45	$d_{zx}(Ir) + \pi(L) + \pi(Cl) + \pi(PPh_3)$
205	H – 4	–6.32	13	1	8	0	76	2	$d_{zx}(Ir) + \pi(PPh_3)$
204	H – 5	–6.58	5	61	13	0	11	10	$\pi(L) + \pi(Cl) + \pi(PPh_3)$

Table S13 Frontier Molecular Orbital Composition (%) in the Excited State for **4**

Orbital	α–MO	Energy (EV)	Contribution (%)						Main Bond Type
			Ir	Ligand			PPh_3	Cl	
				Azo	Ph	SO_2			
225	L + 5	–0.46	14	4	7	1	72	2	$d_{x^2-y^2}$(Ir) + π*(L) + π*(PPh_3)
224	L + 4	–0.62	1	0	28	4	67	0	π*(L) + π*(PPh_3)
223	L + 3	–0.67	0	0	12	2	85	0	π*(L) + π*(PPh_3)
222	L + 2	–0.69	1	0	1	1	94	3	π*(PPh_3)
221	L + 1	–086	30	7	16	9	33	5	$d_{x^2-y^2}$(Ir) + π*(L) + π*(PPh_3)
220	L	–1.65	31	3	2	1	59	4	d_{z^2}(Ir) + π*(PPh_3)
219	H	–3.96	4	47	44	1	3	0	π(L)
218	H – 1	–5.92	6	13	73	3	3	1	π(L)
217	H – 2	–6.11	26	1	21	36	2	14	d_{xy}(Ir) + π(L) + π(Cl)
216	H – 3	–6.26	8	1	73	0	17	0	π(L) + π(PPh_3)
215	H – 4	–6.37	8	0	1	1	82	9	π(PPh_3)
214	H – 5	–6.61	10	0	6	2	60	22	π(PPh_3) + π(Cl)

Orbital	β–MO	Energy (EV)	Contribution (%)						Main Bond Type
			Ir	Ligand			PPh_3	Cl	
				Azo	Ph	SO_2			
223	L + 5	–0.66	0	0	6	1	93	0	π*(PPh_3)
222	L + 4	–0.67	5	1	4	3	85	3	π*(PPh_3)
221	L + 3	–0.74	13	3	6	5	69	3	$d_{x^2-y^2}$(Ir) + π*(L) + π*(PPh_3)
220	L + 2	–1.56	30	3	2	1	61	4	d_{z^2}(Ir) + π*(PPh_3)
219	L + 1	–1.92	2	41	52	1	4	0	π*(L)
218	L	–4.25	34	1	18	37	1	10	$d_{x^2-y^2}$(Ir) + π*(L) + π*(Cl)
217	H	–5.49	6	22	67	2	2	11	π(L) + π(Cl)
216	H – 1	–6.08	10	1	75	1	13	0	π(L) + π(PPh_3)
215	H – 2	–6.35	8	0	2	1	79	9	π(PPh_3)
214	H – 3	–6.55	15	0	10	4	47	24	d_{zx}(Ir) + π(PPh_3) + π(Cl)
213	H – 4	–6.59	16	1	6	13	45	19	d_{xy}(Ir) + π(L) + π(Cl)
212	H – 5	–6.68	1	0	55	7	36	1	π(L) + π(PPh_3)

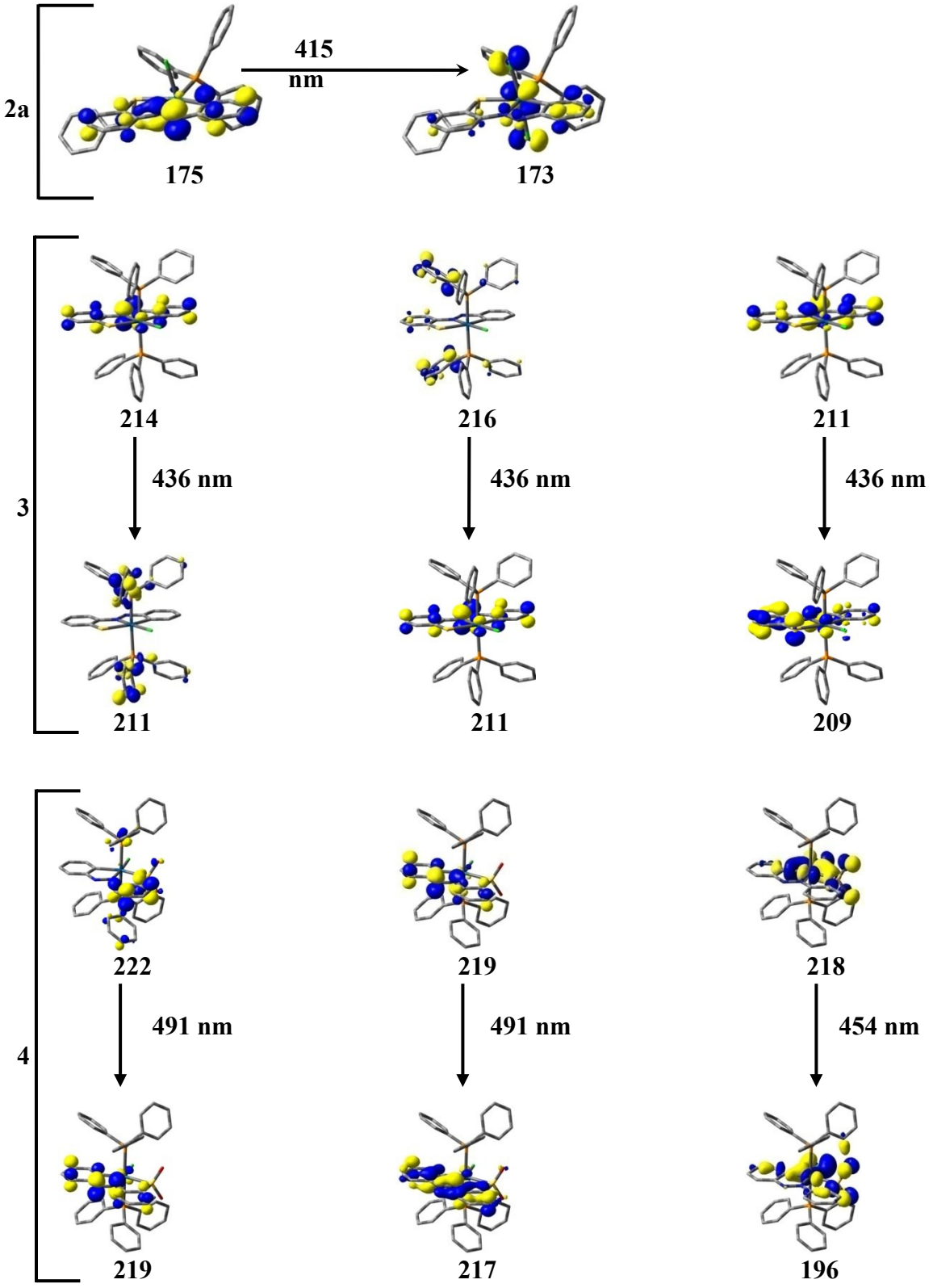

Fig. S15 Frontier molecular orbitals related to emission of **2a**, **3** and **4**.

Table S14 Main calculated vertical transitions with compositions, vertical excitation energies and oscillator strength of **2a, 3** and **4** in dichloromethane based on the lowest lying triplet excited state

Complex	Excitation	Composition	E (eV)	Oscillator strength (*f*)	λ_{theo} (nm)	Assignment	λ_{exp} (nm)
2a	1.	175 → 173 (79%)	2.9866	0.0164	415.13	^{3}LMCT/ILCT/LLCT	442
3	1.	216 → 211 (24%) 211 → 209 (22%) 214 → 211 (11%)	2.8974	0.0307	427.91	LLCT/ILCT/^{3}LMCT	436
4	1.	219 → 217 (65%) 222 → 219 (21%)	2.5247	0.0789	491.09	ILCT/LLCT	439
	2.	218 → 196 (80%)	2.7260	0.0208	454.82	^{3}MLCT	

Table S15 Coordinates of optimized geometry **[1]2a**

Tag	Symbol	X	Y	Z
1	Ir	0.221718	0.873935	-0.0402
2	Cl	-0.24943	0.833551	2.350221
3	Cl	0.419954	1.083002	-2.46491
4	S	-1.99534	-0.18918	-0.59759
5	P	1.605484	-1.07452	-0.04966
6	N	-0.88574	2.595463	-0.1221
7	N	-0.28772	3.723494	0.055359
8	C	1.632085	2.269587	0.374041
9	C	2.980161	2.18938	0.753056
10	H	3.461696	1.224844	0.858082
11	C	3.726068	3.343919	1.031076
12	H	4.767344	3.242793	1.32387
13	C	3.154529	4.62633	0.945806
14	H	3.751063	5.506055	1.160475
15	C	1.814164	4.749578	0.60187
16	H	1.3231	5.714791	0.545928
17	C	1.066685	3.585936	0.333323
18	C	-2.27383	2.596637	-0.42309
19	C	-3.00116	3.796156	-0.51407
20	H	-2.48492	4.728334	-0.32669
21	C	-4.35307	3.766811	-0.84752
22	H	-4.90828	4.696131	-0.916
23	C	-4.98912	2.545925	-1.11104
24	H	-6.03718	2.523352	-1.38953
25	C	-4.26839	1.350771	-1.02962
26	H	-4.75127	0.40772	-1.25331
27	C	-2.91409	1.36186	-0.66449
28	C	-2.69141	-1.02934	0.930012
29	H	-1.98614	-1.8563	1.06727
30	H	-2.56599	-0.33966	1.764983
31	C	-4.10685	-1.52022	0.786178
32	C	-4.41753	-2.60434	-0.05631
33	H	-3.62337	-3.0909	-0.61582
34	C	-5.73421	-3.05778	-0.17489
35	H	-5.9597	-3.89576	-0.82713
36	C	-6.7612	-2.43723	0.549681
37	H	-7.78299	-2.79181	0.458601
38	C	-6.4622	-1.36316	1.394632
39	H	-7.25111	-0.88105	1.963336
40	C	-5.14373	-0.90675	1.510237
41	H	-4.9141	-0.07352	2.16784
42	C	2.481907	-1.49192	1.520985
43	C	1.744562	-1.74044	2.697761
44	H	0.66493	-1.67142	2.68585
45	C	2.397447	-2.04135	3.896992
46	H	1.811621	-2.22654	4.791433
47	C	3.795363	-2.08431	3.949373
48	H	4.299667	-2.3104	4.883518

49	C	4.538165	-1.82793	2.792926
50	H	5.622852	-1.85556	2.822878
51	C	3.888631	-1.53807	1.586744
52	H	4.481081	-1.35276	0.698916
53	C	2.955018	-1.14586	-1.31143
54	C	3.48319	-2.39569	-1.69786
55	H	3.075456	-3.31029	-1.28112
56	C	4.52799	-2.47258	-2.62335
57	H	4.920112	-3.44279	-2.91168
58	C	5.061436	-1.30278	-3.17891
59	H	5.868828	-1.36254	-3.90202
60	C	4.543546	-0.0595	-2.80424
61	H	4.940291	0.851731	-3.23971
62	C	3.495221	0.021401	-1.87869
63	H	3.085012	0.987495	-1.62178
64	C	0.648799	-2.60383	-0.47734
65	C	0.572883	-3.74036	0.347802
66	H	1.090633	-3.75943	1.298995
67	C	-0.16075	-4.86523	-0.05537
68	H	-0.2086	-5.73329	0.594653
69	C	-0.81632	-4.87433	-1.2903
70	H	-1.37676	-5.74929	-1.60441
71	C	-0.73747	-3.75076	-2.12509
72	H	-1.23532	-3.75053	-3.08951
73	C	-0.01499	-2.62271	-1.72393
74	H	0.039058	-1.75877	-2.37916

Table S16 Coordinates of optimized geometry **[1]3**

Tag	Symbol	X	Y	Z
1	Ir	0.240648	0.17532	0.000000
2	Cl	2.102631	1.806562	0.000000
3	S	-1.756130	1.71216	0.000000
4	P	0.260119	0.294069	2.433252
5	N	-1.17346	-1.26716	0.000000
6	N	-0.80958	-2.51455	0.000000
7	C	1.409939	-1.51975	0.000000
8	C	2.794283	-1.73916	0.000000
9	H	3.469243	-0.89167	0.000000
10	C	3.32113	-3.03952	0.000000
11	H	4.398815	-3.17724	0.000000
12	C	2.481074	-4.16684	0.000000
13	H	2.906332	-5.16495	0.000000
14	C	1.099996	-3.99142	0.000000
15	H	0.41613	-4.83391	0.000000
16	C	0.577976	-2.68318	0.000000
17	C	-2.55751	-0.96061	0.000000
18	C	-3.52644	-1.9858	0.000000
19	H	-3.18827	-3.01362	0.000000
20	C	-4.87599	-1.6653	0.000000
21	H	-5.62216	-2.45267	0.000000
22	C	-5.27014	-0.31176	0.000000
23	H	-6.32552	-0.05558	0.000000
24	C	-4.31858	0.700562	0.000000
25	H	-4.6242	1.741297	0.000000
26	C	-2.93346	0.407094	0.000000
27	C	0.199412	1.966899	3.220712
28	C	0.21345	2.047195	4.629496
29	H	0.255758	1.142415	5.225922
30	C	0.178741	3.286526	5.272524
31	H	0.187411	3.329935	6.357103
32	C	0.140332	4.466931	4.519163
33	H	0.117401	5.430723	5.0183
34	C	0.138804	4.39741	3.12359
35	H	0.118115	5.306422	2.531369
36	C	0.167624	3.155771	2.475553
37	H	0.185036	3.112584	1.397733
38	C	1.726848	-0.43133	3.303899
39	C	1.616923	-1.26538	4.432859
40	H	0.644019	-1.56931	4.798173
41	C	2.762311	-1.70978	5.10491
42	H	2.656483	-2.35486	5.971745
43	C	4.031908	-1.32099	4.667972
44	H	4.918648	-1.66424	5.191788
45	C	4.150951	-0.48131	3.554614
46	H	5.131604	-0.16713	3.211133

47	C	3.01152	-0.03998	2.875762
48	H	3.113485	0.613848	2.017638
49	C	-1.19165	-0.57814	3.157675
50	C	-2.31339	0.139815	3.61305
51	H	-2.31129	1.22234	3.584281
52	C	-3.43954	-0.53454	4.098422
53	H	-4.29633	0.035489	4.442953
54	C	-3.46374	-1.93203	4.13601
55	H	-4.33733	-2.45281	4.515143
56	C	-2.35961	-2.65682	3.672196
57	H	-2.37349	-3.74198	3.686148
58	C	-1.23531	-1.98782	3.179642
59	H	-0.39444	-2.56473	2.811847
60	P	0.260119	0.294069	-2.43325
61	C	0.199412	1.966899	-3.22071
62	C	0.21345	2.047195	-4.6295
63	H	0.255758	1.142415	-5.22592
64	C	0.178741	3.286526	-5.27252
65	H	0.187411	3.329935	-6.3571
66	C	0.140332	4.466931	-4.51916
67	H	0.117401	5.430723	-5.0183
68	C	0.138804	4.39741	-3.12359
69	H	0.118115	5.306422	-2.53137
70	C	0.167624	3.155771	-2.47555
71	H	0.185036	3.112584	-1.39773
72	C	1.726848	-0.43133	-3.3039
73	C	1.616923	-1.26538	-4.43286
74	H	0.644019	-1.56931	-4.79817
75	C	2.762311	-1.70978	-5.10491
76	H	2.656483	-2.35486	-5.97174
77	C	4.031908	-1.32099	-4.66797
78	H	4.918648	-1.66424	-5.19179
79	C	4.150951	-0.48131	-3.55461
80	H	5.131604	-0.16713	-3.21113
81	C	3.01152	-0.03998	-2.87576
82	H	3.113485	0.613848	-2.01764
83	C	-1.19165	-0.57814	-3.15768
84	C	-2.31339	0.139815	-3.61305
85	H	-2.31129	1.22234	-3.58428
86	C	-3.43954	-0.53454	-4.09842
87	H	-4.29633	0.035489	-4.44295
88	C	-3.46374	-1.93203	-4.13601
89	H	-4.33733	-2.45281	-4.51514
90	C	-2.35961	-2.65682	-3.6722
91	H	-2.37349	-3.74198	-3.68615
92	C	-1.23531	-1.98782	-3.17964
93	H	-0.39444	-2.56473	-2.81185

Table S17 Coordinates of optimized geometry $^{2}\mathbf{3}^{\bullet+}$

Tag	Symbol	X	Y	Z
1	Ir	0.182489	0.20846	0.000015
2	Cl	2.019953	1.826651	0.000044
3	S	-1.72282	1.713916	0.000002
4	P	0.27633	0.283003	2.485831
5	N	-1.23919	-1.22013	0.000015
6	N	-0.88245	-2.47598	0.000020
7	C	1.327463	-1.47186	0.000035
8	C	2.714321	-1.68716	0.000087
9	H	3.386938	-0.83957	0.00012
10	C	3.233823	-2.98522	0.000108
11	H	4.310028	-3.12671	0.000146
12	C	2.391605	-4.12122	0.000083
13	H	2.825129	-5.11469	0.000102
14	C	1.015791	-3.9575	0.000049
15	H	0.336175	-4.8023	0.000042
16	C	0.487418	-2.64471	0.000031
17	C	-2.61266	-0.90354	0.000022
18	C	-3.61251	-1.88949	0.000037
19	H	-3.32131	-2.93104	0.000043
20	C	-4.95091	-1.50709	0.000045
21	H	-5.7246	-2.26666	0.000057
22	C	-5.3086	-0.14277	0.000038
23	H	-6.35491	0.141584	0.000045
24	C	-4.3251	0.838696	0.000024
25	H	-4.59107	1.88963	0.000019
26	C	-2.9567	0.478779	0.000016
27	C	0.19682	1.952035	3.262673
28	C	0.230115	2.018989	4.673237
29	H	0.303904	1.111457	5.26238
30	C	0.17248	3.252121	5.325067
31	H	0.19609	3.287726	6.409019
32	C	0.092266	4.437748	4.582141
33	H	0.052972	5.395481	5.090159
34	C	0.075634	4.38183	3.186318
35	H	0.0318	5.295812	2.603873
36	C	0.130269	3.146698	2.527257
37	H	0.164837	3.122848	1.448326
38	C	1.76969	-0.44668	3.281902
39	C	1.692809	-1.34903	4.360836
40	H	0.734364	-1.69746	4.723402
41	C	2.858799	-1.7956	4.994281
42	H	2.782377	-2.48964	5.824778
43	C	4.111262	-1.34222	4.569441
44	H	5.012371	-1.68595	5.066359
45	C	4.195217	-0.43199	3.509088
46	H	5.162055	-0.06259	3.183368
47	C	3.036749	0.014443	2.867714
48	H	3.112754	0.727006	2.055223

49	C	-1.16875	-0.61264	3.188973
50	C	-2.28439	0.09452	3.679324
51	H	-2.27643	1.177641	3.699558
52	C	-3.40517	-0.59169	4.161259
53	H	-4.25107	-0.03093	4.544664
54	C	-3.43103	-1.99	4.160037
55	H	-4.29626	-2.51982	4.544248
56	C	-2.33303	-2.70361	3.66403
57	H	-2.34431	-3.78853	3.660283
58	C	-1.21343	-2.0232	3.17602
59	H	-0.373	-2.59338	2.797514
60	P	0.276334	0.283028	-2.48581
61	C	0.196507	1.952047	-3.26265
62	C	0.229998	2.019021	-4.67321
63	H	0.30412	1.111514	-5.26235
64	C	0.17214	3.252144	-5.32504
65	H	0.19591	3.287762	-6.40898
66	C	0.091497	4.437743	-4.58211
67	H	0.052028	5.395469	-5.09013
68	C	0.074656	4.381808	-3.18629
69	H	0.030482	5.295774	-2.60385
70	C	0.129515	3.146687	-2.52723
71	H	0.163904	3.122836	-1.4483
72	C	1.769811	-0.44639	-3.28189
73	C	1.693044	-1.34899	-4.36062
74	H	0.734647	-1.69778	-4.72297
75	C	2.859079	-1.79537	-4.99411
76	H	2.782747	-2.48961	-5.82445
77	C	4.111468	-1.34155	-4.56953
78	H	5.012611	-1.68513	-5.06649
79	C	4.195303	-0.43107	-3.50938
80	H	5.162078	-0.06132	-3.18386
81	C	3.036791	0.01517	-2.86795
82	H	3.112696	0.727936	-2.05563
83	C	-1.16856	-0.61289	-3.18899
84	C	-2.28445	0.094035	-3.67909
85	H	-2.27684	1.177163	-3.69908
86	C	-3.40507	-0.59242	-4.16108
87	H	-4.25118	-0.03184	-4.54428
88	C	-3.43049	-1.99073	-4.16018
89	H	-4.29559	-2.52074	-4.54444
90	C	-2.33221	-2.70412	-3.66445
91	H	-2.34314	-3.78904	-3.66096
92	C	-1.21278	-2.02346	-3.17637
93	H	-0.37212	-2.59347	-2.79811

Table S18 Coordinates of optimized geometry **[1]4**

Tag	Symbol	X	Y	Z
1	Ir	0.198789	0.150314	0.000000
2	P	0.283228	0.254124	2.466653
3	S	-1.89572	1.46501	0.000000
4	Cl	1.938031	1.88595	0.000000
5	O	-2.27669	2.199877	-1.27242
6	N	-1.07197	-1.43369	0.000000
7	N	-0.58535	-2.63625	0.000000
8	C	1.513024	-1.42695	0.000000
9	C	2.913689	-1.50614	0.000000
10	H	3.498186	-0.59489	0.000000
11	C	3.564247	-2.7457	0.000000
12	H	4.649981	-2.77652	0.000000
13	C	2.841158	-3.95622	0.000000
14	H	3.367714	-4.90442	0.000000
15	C	1.453485	-3.92294	0.000000
16	H	0.858121	-4.82989	0.000000
17	C	0.803571	-2.66888	0.000000
18	C	-2.48971	-1.28617	0.000000
19	C	-3.35423	-2.39782	0.000000
20	H	-2.93263	-3.39386	0.000000
21	C	-4.73018	-2.19031	0.000000
22	H	-5.39983	-3.044	0.000000
23	C	-5.25579	-0.88609	0.000000
24	H	-6.33016	-0.73375	0.000000
25	C	-4.39676	0.213769	0.000000
26	H	-4.7818	1.227289	0.000000
27	C	-3.01241	0.013617	0.000000
28	C	0.315975	1.903831	3.298074
29	C	0.189404	3.120893	2.612194
30	H	0.038962	3.13112	1.546002
31	C	0.244648	4.333243	3.312026
32	H	0.142744	5.264556	2.76531
33	C	0.421023	4.344808	4.697678
34	H	0.461197	5.287093	5.235279
35	C	0.546579	3.134454	5.391931
36	H	0.685378	3.131902	6.468477
37	C	0.50061	1.923346	4.697863
38	H	0.613344	0.994526	5.246912
39	C	-1.14859	-0.61565	3.230355
40	C	-2.21672	0.121978	3.77739
41	H	-2.19735	1.20363	3.749461
42	C	-3.32653	-0.53718	4.318985
43	H	-4.14245	0.047041	4.731657
44	C	-3.38934	-1.93433	4.321866
45	H	-4.24972	-2.44131	4.747193
46	C	-2.34321	-2.67613	3.760835
47	H	-2.389	-3.76048	3.744817
48	C	-1.2354	-2.02397	3.210153

49	H	-0.4454	-2.61644	2.762803
50	C	1.796866	-0.4987	3.227022
51	C	1.769506	-1.51016	4.20386
52	H	0.830047	-1.93944	4.526589
53	C	2.957633	-1.96315	4.793282
54	H	2.915143	-2.74474	5.545575
55	C	4.185273	-1.40549	4.427093
56	H	5.103551	-1.754	4.889293
57	C	4.220991	-0.38578	3.46778
58	H	5.167612	0.063069	3.183673
59	C	3.040742	0.064174	2.871134
60	H	3.078984	0.857057	2.132836
61	O	-2.27669	2.199877	1.272417
62	P	0.283228	0.254124	-2.46665
63	C	0.315975	1.903831	-3.29807
64	C	0.189404	3.120893	-2.61219
65	H	0.038962	3.13112	-1.546
66	C	0.244648	4.333243	-3.31203
67	H	0.142744	5.264556	-2.76531
68	C	0.421023	4.344808	-4.69768
69	H	0.461197	5.287093	-5.23528
70	C	0.546579	3.134454	-5.39193
71	H	0.685378	3.131902	-6.46848
72	C	0.50061	1.923346	-4.69786
73	H	0.613344	0.994526	-5.24691
74	C	-1.14859	-0.61565	-3.23036
75	C	-2.21672	0.121978	-3.77739
76	H	-2.19735	1.20363	-3.74946
77	C	-3.32653	-0.53718	-4.31899
78	H	-4.14245	0.047041	-4.73166
79	C	-3.38934	-1.93433	-4.32187
80	H	-4.24972	-2.44131	-4.74719
81	C	-2.34321	-2.67613	-3.76084
82	H	-2.389	-3.76048	-3.74482
83	C	-1.2354	-2.02397	-3.21015
84	H	-0.4454	-2.61644	-2.7628
85	C	1.796866	-0.4987	-3.22702
86	C	1.769506	-1.51016	-4.20386
87	H	0.830047	-1.93944	-4.52659
88	C	2.957633	-1.96315	-4.79328
89	H	2.915143	-2.74474	-5.54558
90	C	4.185273	-1.40549	-4.42709
91	H	5.103551	-1.754000	-4.88929
92	C	4.220991	-0.38578	-3.46778
93	H	5.167612	0.063069	-3.18367
94	C	3.040742	0.064174	-2.87113
95	H	3.078984	0.857057	-2.13284